agriculture

MDPI

*Article*

# Evolution and Modelling of the Moisture Diffusion in Walnuts during the Combination of Hot Air and Microwave–Vacuum Drying

**Xiaolan Man [1], Long Li [1], Xiuwen Fan [1,2,3,*], Hong Zhang [1,2,3], Haipeng Lan [1,2,3], Yurong Tang [1,2,3] and Yongcheng Zhang [1,2,3]**

[1] College of Mechanical Electrification Engineering, Tarim University, Alar 843300, China; 10757202202@stumail.taru.edu.cn (X.M.)
[2] Key Laboratory of Modern Agricultural Engineering, Tarim University, Alar 843300, China
[3] Key Laboratory of Tarim Oasis Agriculture, Tarim University, Ministry of Education, Alar 843300, China
* Correspondence: fanxiuwen@taru.edu.cn; Tel.: +86-138-9920-6653

**Abstract:** To understand the moisture transfer mechanism of walnuts during the combination of hot air (*HA*) and microwave–vacuum (*MV*) drying (*HA-MVD*) process, the drying characteristics and moisture diffusion characteristics of walnut during *HA-MVD* were investigated. The results indicated that the *HA-MVD* of walnuts occurred mainly in the falling-rate stage. The value of effective moisture diffusivity ($D_{eff}$) dropped continuously with the decrease in moisture content (*MC*) during the *HA* drying, while switching to *MV* drying could truncate the decrease in $D_{eff}$ and still maintain a high value until the end of drying. The *HA* temperature, *MC* of the transition point, microwave power, and *MV* thermostatic temperature have significant effects on the moisture diffusion characteristics of walnuts. The values of $D_{eff}$ for walnuts ranged from $2.33 \times 10^{-9}$ $m^2/s$ to $6.89 \times 10^{-8}$ $m^2/s$. The third-order polynomial prediction model of $D_{eff}$ related to the sample *MC* and drying conditions was established to describe the dynamic change in the $D_{eff}$ of walnuts during the *HA-MVD* process. The application of *MVD* in the final stage of drying could rapidly increase the internal vapor pressure of the walnuts, accelerate the diffusion speed of the internal moisture, and re-enhance the drying rate. The findings have practical value for the development of efficient and energy-saving drying methods in the walnut industry.

**Keywords:** walnut; combined drying; hot air drying; microwave–vacuum drying; moisture diffusion; model

check for updates

**Citation:** Man, X.; Li, L.; Fan, X.; Zhang, H.; Lan, H.; Tang, Y.; Zhang, Y. Evolution and Modelling of the Moisture Diffusion in Walnuts during the Combination of Hot Air and Microwave–Vacuum Drying. *Agriculture* **2024**, *14*, 190. https://doi.org/10.3390/agriculture14020190

Academic Editor: Perla A. Gómez

Received: 7 December 2023
Revised: 20 January 2024
Accepted: 24 January 2024
Published: 26 January 2024

**Copyright:** © 2024 by the authors. Licensee MDPI, Basel, Switzerland. This article is an open access article distributed under the terms and conditions of the Creative Commons Attribution (CC BY) license (https://creativecommons.org/licenses/by/4.0/).

## 1. Introduction

Walnuts are important economic crops and have attracted increasing attention for their multiple health benefits and extensive applications in food, chemistry, and medicine [1–3]. The walnut kernel has a large number of nutrients, mainly including proteins, fats, amino acids, minerals, and vitamins, with a high unsaturated fatty acid content of more than 50% and a protein content of 20% [4,5]. Freshly harvested walnuts typically have a high initial moisture content (*IMC*) and physiological activity [6,7]. Such characteristics make fresh walnuts susceptible to contamination by bacteria during storage [8]. As a result, drying is an essential step in the primary processing of fresh walnuts to remove water, avoid microbial spoilage, and maintain the quality [9,10]. Meanwhile, it can also reduce transportation weight and storage costs, and increase consumption diversity. Currently, hot air drying (*HAD*) is still predominantly used in industrial walnut production due to processing ability and running costs [11]. However, *HAD* of whole walnuts is time consuming because of their hard and thick shell, which prevents heat and mass transfer [12]. Thus, there is an urgent need for new drying approaches to specifically improve the drying process of walnut.

Microwave drying (*MD*), as a volumetric heating method, is characterized by high heating efficiency, high processing capacity and easy controllability [13,14]. Therefore, using *MD* instead of *HAD* can reduce the drying time and improve the product properties [15–17]. Microwave–vacuum drying (*MVD*) overcomes the shortcomings of *MD* alone, e.g., uneven heating of food materials with a high *MC* or difficulties in controlling the temperature of the materials [18,19]. Previous studies have shown that the application of *MVD* at the final drying stage could rapidly increase the internal vapor pressure of the food, accelerate the migration of the internal moisture, and re-enhance the drying rate, which would give the advantages of shortening the drying time and ensuring product quality [20,21]. The combination of hot air (*HA*) and microwave–vacuum (*MV*) drying (*HA-MVD*) is an emerging method of drying and it is suitable for drying different food and agriculture materials due to its high drying efficiency, low energy consumption, and good product quality [21–23]. However, to the best of our knowledge, no reports have been published studying the *HA-MVD* of walnut or other similar tree nuts.

Many researchers have studied the *HA-MVD* of food materials. Zhou et al. investigated the changes in *MC* and quality properties of cranberries under *HA-MVD* [21]; Wu et al. discussed the effects of *IMC*, microwave intensity, microwave irradiation time, and vacuum degree on the product quality of puffed duck breast and determined the optimal combination of *HA-MVD* process parameters [24]; Figiel researched the drying kinetics and quality properties of beetroots under *HA-MVD* [22]. However, most of these studies have focused on drying characteristics, kinetics, quality, and process, and few systematic reports have been made on the internal moisture diffusion characteristics during *HA-MVD*, which is very important for understanding and accurately grasping the *HA-MVD* process for foods. The moisture diffusion of food materials is usually greatly affected by drying conditions and sample moisture content (*MC*), but previous studies on the moisture diffusion in food materials were performed based on the assumption that effective moisture diffusivity ($D_{eff}$) remains constant throughout the drying process, which usually does not yield relevant information about the internal moisture dynamic diffusion of materials during the *HA-MVD* process [25–28]. Bal et al. found a significant correlation between the $D_{eff}$ and *MC*s of bamboo shoot slices during the *MD* process [29]. Dadalı et al. determined the $D_{eff}$ of okra under *MD* and established it as third-order polynomial function of *MC* [30]. Nevertheless, until now, limited documented information is available on the evolution of the moisture diffusion characteristics of walnuts during *HA-MVD*, and in particular, the relationship between $D_{eff}$ and sample *MC* and the drying conditions has not been clarified.

Therefore, this paper takes walnuts as the research object, studies the change pattern of moisture and $D_{eff}$ during the *HA-MVD* process of walnuts, explores the influence of *HA* temperature, the *MC* of the transition point, microwave power, and *MV* thermostatic temperature on the drying characteristics and internal moisture diffusion characteristics of walnuts, and constructs a mathematical model of $D_{eff}$ related to the MC and drying conditions. This study provides (i) an improved understanding of moisture transfer mechanisms during the *HA-MVD* drying of walnuts and (ii) a theoretical reference for applying *HA-MVD* technology to drying walnuts and other similar nuts.

## 2. Materials and Methods

### *2.1. Material Preparation*

Fresh walnut samples of the Wen-185 variety were bought in 2023. All walnut samples were vacuum-packed in 30 plastic bags, each of which weighed 4.50 ± 0.01 kg, and were stored in an air-conditioned room at a relative humidity of 60% and a temperature of 21 °C to prevent water loss [31]. Walnut samples with similar dimensions and weights were selected for testing to reduce the variation in *IMC* and improve the representativeness of the sample selection [32]. The *IMC* of walnut samples was measured using an *HA* dryer at 105 ± 1 °C for 24 h according to Equation (1) [14]:

$$IMC = \frac{W_0 - W_e}{W_0} \times 100\% \quad (1)$$

where $W_e$ and $W_0$ are the dry and initial masses of the sample, respectively (g). The *IMC* of the walnuts is 41.43 ± 1.25% on a wet basis (w.b.).

### 2.2. Drying Equipment

The experimental equipment primarily consists of an *HA* dryer (BoXun, GZX-9140MBE, Shanghai, China) and an *MV* dryer (Huaiteng, HTWB-01, Nanjing, China) (Figure 1). The *MV* dryer was equipped with an infrared temperature sensor (Opus, RT-350 °C, Stamford, Germany) for real-time monitoring of the surface temperature of the samples. To ensure product quality and reduce energy consumption, a drying strategy is used in which the microwave can only operate below the maximum temperature set by the system, and when the temperature exceeds the maximum temperature, the microwave is automatically turned off [21,33]. The vacuum was set at −0.08 MPa. In order to improve the uniformity of microwave drying, the samples were rotated on the turntable at a speed of 6 rpm during the *MVD* process [14,34,35].

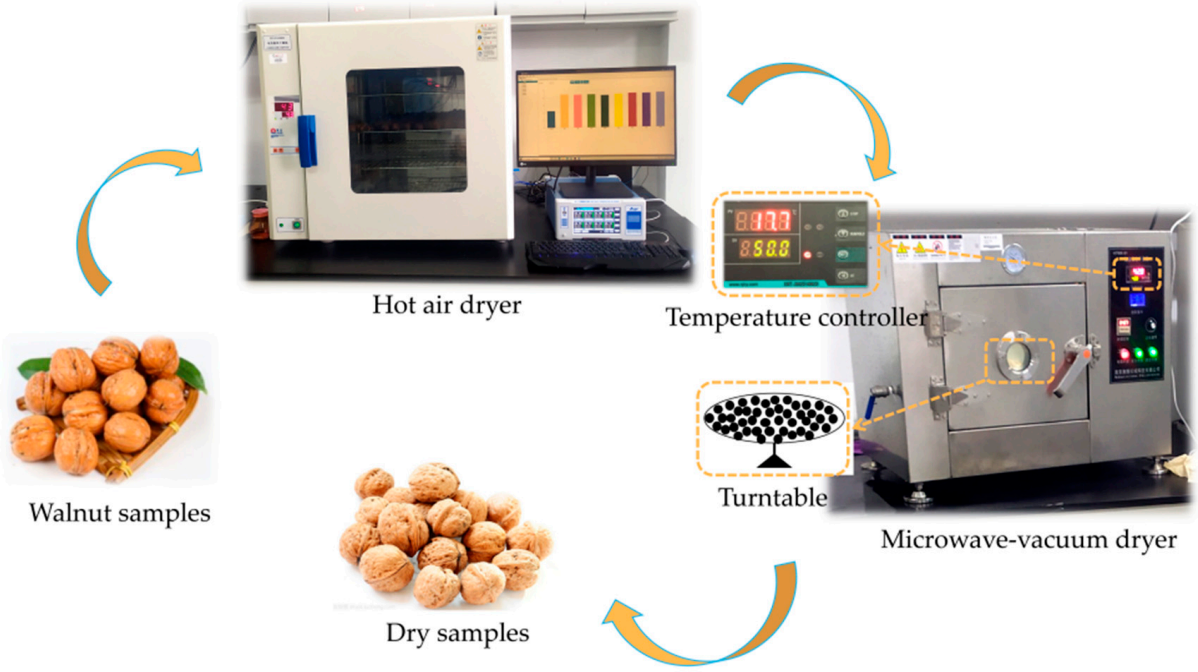



**Figure 1.** Diagram of the *HA-MVD* system.

### 2.3. Drying Experiments

A fix three variables to change one variable design was used in the experimental scheme. The detailed plans of the *HA-MVD* test for walnuts are summarised in Table 1.

The *HAD* oven was turned on to preheat, and after the system reached thermal equilibrium, the walnuts were rapidly placed on a *HA* dryer for drying. The *HAD* stage was stopped when the *MC* of the walnut reached the *MC* at the transition point (36, 30, 24, 18 and 14%). The walnuts were then rapidly transferred to the *MVD* stage [21]. Note that the sample experimental steps should be completed within 5 s to improve the accuracy of the test results [20]. To track the *MC* variation in the walnuts during the *HA-MVD*, we swiftly removed the 30 marked walnuts from the dryer, and the weight of each sample was measured on a digital balance (Anting, FA1104, Shanghai, China), and they were then put back until the end of drying. For all walnut drying tests, three replicates were performed.

**Table 1.** Details of operating parameters for the *HA-MVD* experimental.

| Test No. | Hot Air Temperature (°C) | Moisture Content at the Transition Point (%) | Microwave Power (W) | Microwave–Vacuum Thermostatic Temperature (°C) |
|---|---|---|---|---|
| 1 | 45 | 30 | 600 | 50 |
| 2 | 60 | 30 | 600 | 50 |
| 3 | 75 | 30 | 600 | 50 |
| 4 | 90 | 30 | 600 | 50 |
| 5 | 105 | 30 | 600 | 50 |
| 6 | 60 | 36 | 600 | 50 |
| 7 | 60 | 30 | 600 | 50 |
| 8 | 60 | 24 | 600 | 50 |
| 9 | 60 | 18 | 600 | 50 |
| 10 | 60 | 14 | 600 | 50 |
| 11 | 60 | 30 | 200 | 50 |
| 12 | 60 | 30 | 400 | 50 |
| 13 | 60 | 30 | 600 | 50 |
| 14 | 60 | 30 | 800 | 50 |
| 15 | 60 | 30 | 1000 | 50 |
| 16 | 60 | 30 | 600 | 30 |
| 17 | 60 | 30 | 600 | 40 |
| 18 | 60 | 30 | 600 | 50 |
| 19 | 60 | 30 | 600 | 60 |
| 20 | 60 | 30 | 600 | 70 |

### 2.4. Drying Characteristic Parameters

The moisture ratio of the walnuts was calculated using Equation (2) [25]:

$$MR = \frac{M_t - M_\infty}{IMC - M_\infty} \quad (2)$$

where $M_\infty$ and $M_t$ are the $MC$ at the drying end (%) and the $MC$ at time $t$ (%), respectively.

The drying rate of the walnuts was calculated using Equation (3) [9]:

$$DR = \frac{M_t - M_{t+\Delta t}}{\Delta t} \quad (3)$$

where $DR$ is the drying rate (%/min); $M_{t+\Delta t}$ is the $MC$ of the walnuts at time $t + \Delta t$ (%); $\Delta t$ is the time difference between $t + \Delta t$ and $t$.

### 2.5. Effective Moisture Diffusivity

The $D_{eff}$ is the most important key parameter required for the analysis of intrinsic moisture diffusion characteristics during the biological or food material drying process [36,37]. When the drying of rectangular, spherical, and other shapes of materials is mainly controlled by the descending drying stage, Fick's second law can be adopted to analyse the process of moisture diffusion inside the material [32,38]. Generally, the walnut has been viewed as a sphere in the theoretical research due to its relatively high sphericity and axially symmetry [9,39]. Therefore, the walnuts were treated as spheres in this study.

The $D_{eff}$ of walnut at corresponding $MC$s under different drying conditions was calculated based on the Fick's diffusion equation by assuming a spherical shape with negligible volumetric shrinkage [9,32]. Similar to those made in previous studies [9,29,32,40], the following important assumptions were made:

(1) In the beginning, the moisture was evenly distributed throughout the mass of the sphere;

(2) In relation to the centre of the sphere, the mass transfer was symmetrical;

(3) Compared to the internal resistance of the walnut sample, the surface mass transfer resistance was negligible;

(4) $D_{eff}$ was constant only within the short time interval between the two adjacent measuring points and was piecewise continuous throughout the whole drying process.

Note that assumption (4) was proposed in order to compensate for the inaccuracy due to the constant diffusivity [32].

The general form of the Fick's second law is expressed as [32]:

$$\frac{\partial MC}{\partial t} = \frac{\partial}{\partial r}\left(D_{eff}\frac{\partial MC}{\partial r}\right) \tag{4}$$

Crank proposed the analytical solution of this partial differential equation for the one-dimensional moisture transfer in spherical geometry in the way that infinite series [9,41]:

$$MR = \frac{M_t - M_e}{M_0 - M_e} = \frac{6}{\pi^2}\sum_{n=1}^{\infty}\frac{1}{n^2}\exp\left(-\frac{n^2\pi^2 D_{eff}t}{r^2}\right) \tag{5}$$

where $n$ is the number of terms; $t$ is the drying time (s); $r$ is the geometric radius (m); $D_{eff}$ is the effective moisture diffusivity of the samples ($m^2 \cdot s^{-1}$).

For long drying times $n$ = 1, then Equation (5) can be simplified to the following form [29,40]:

$$MR = \frac{6}{\pi^2}\exp\left(-\frac{\pi^2 D_{eff}t}{r^2}\right) \tag{6}$$

The $r$ can be calculated as [42]:

$$r = \frac{\sqrt[3]{L \cdot W \cdot T}}{2} \tag{7}$$

where, $L$, $W$ and $T$ are length (m), width (m), and thickness (m), respectively.

The conversion of Equation (7) can be obtained as follows:

$$\ln(MR) = \ln\frac{6}{\pi^2} - \frac{\pi^2 D_{eff}t}{r^2} \tag{8}$$

Then, the $D_{eff}$ can be calculated using Equation (9) [29,40,43]:

$$D_{eff} = \frac{-0.101 \cdot \ln(MR) - 0.0504}{(t/r^2)} \tag{9}$$

The $D_{eff}$ was calculated at each corresponding $MC$ in this study. The average $D_{eff}$ ($D_{eff,ave}$) was determined as an arithmetic average of all $D_{eff}$ values at different $MC$ [32,43]:

$$D_{eff,ave} = \frac{1}{n}\left(\sum_{1}^{n} D_{eff}\right) \tag{10}$$

The mathematical relationship between $D_{eff}$ and sample $MC$ and the drying conditions was developed with polynomial equations as Equation (11) [29,32,40].

$$D_{eff} = A \cdot MC^3 + B \cdot MC^2 + C \cdot MC + D \tag{11}$$

where, $A$, $B$, $C$, and $D$ are the coefficients of the third-order polynomial relationship.

### *2.6. Statistical Analysis*

The determination coefficient ($R^2$) is the most important indicator for evaluating the fit of the model and is used to indicate the close relationship between the variables. The residual sum of squares ($RSS$) reflects the degree of variation between the actual values and the expected values, so that these two criteria can be used to determine the optimal $D_{eff}$ models and to judge the models' merits. A higher quality of fit was associated with a lower

*RSS* and higher $R^2$ [25,29]. Note that the nonlinear regression kit in the Origin software (version 2022) was used to fit regression parameters in the $D_{eff}$ model.

$$R^2 = \frac{\sum_{i=1}^{N}(MR_i - MR_{\text{pre},i})(MR_i - MR_{\text{exp},i})}{\sqrt{\left[\sum_{i=1}^{N}(MR_i - MR_{\text{pre},i})^2\right]\left[\sum_{i=1}^{N}(MR_i - MR_{\text{exp},i})^2\right]}} \quad (12)$$

$$RSS = \sum_{i=1}^{N}(MR_{\text{pre},i} - MR_{\text{exp},i})^2 \quad (13)$$

where $MR_{\text{exp},i}$, $MR_{\text{pre},i}$, and $MR_i$ are experimental *MR*, predicted *MR*, and the average of the experimental *MR*, respectively; *N* is the total data.

## 3. Results and Discussion

### *3.1. Drying Characteristics*

#### 3.1.1. Effect of Hot Air Temperature on Drying Characteristics

In order to investigate the effects of *HA* temperatures of 45, 60, 75, 90, and 105 °C on the drying characteristics at an *MC* at the transition point of 30%, a microwave power of 600 W, and an *MV* thermostatic temperature of 50 °C, the drying curves and drying rate curves of walnut at different *HA* temperatures are shown in Figure 2A,B. As shown in Figure 2A, the *MC*s of walnuts decayed exponentially in two stages during the drying time: the *HAD* and *MVD* stages, which were commonly observed for combined drying of food materials [20–24]. The *MVD* stage was much shorter than the *HAD* stage. The *HAD* stage took from 50 to 195 min, while the *MVD* stage only took from 25 to 30 min (Table 2). When the *HA* temperature was 45, 60, 75, 90, and 105 °C, the total drying time for walnuts was 225, 165, 103, 85, and 77 min, respectively (Table 2). The results showed that, when the *HA* temperature increased from 45 °C to 105 °C, the total drying time for walnuts decreased by 65.78%.

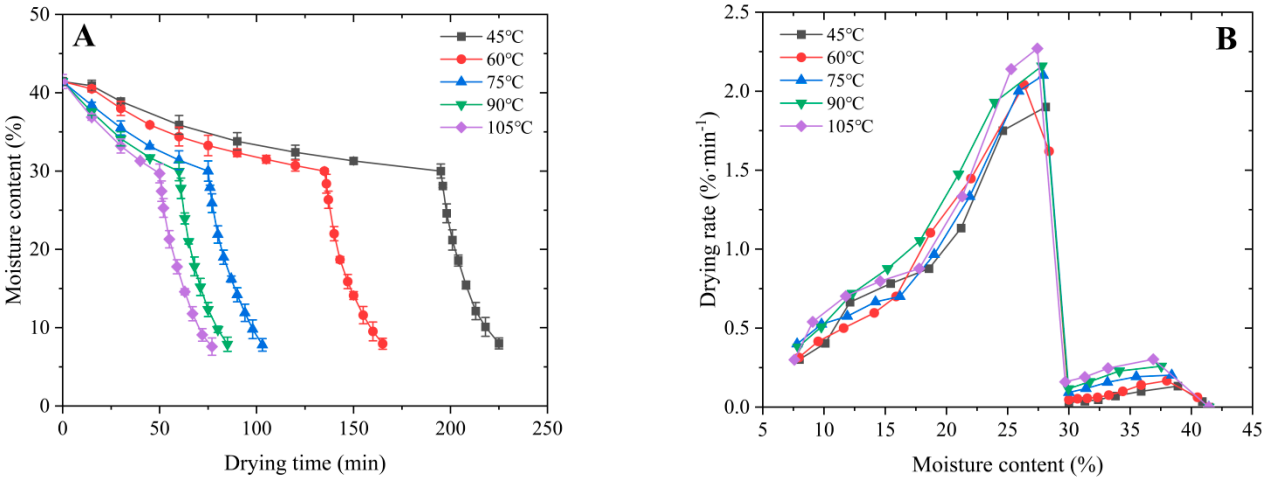



**Figure 2.** (**A**) Drying curves and (**B**) drying rate curves of walnuts at different hot air temperatures.

It can be seen from Figure 2B that the *HAD* stage had significant preheating and falling-rate drying periods, but the average drying rate was very small, about 0.516 to 0.758%/min (Table 2). When the *HAD* reached the *MC* of the transition point, the drying process converted to *MVD*. The drying rate of the walnut increased significantly, which may be attributed to the fact that the use of electromagnetic radiation under reduced pressure could significantly accelerate water transfer [16,19,44]. In addition, it was found that the maximum drying rate in the *HAD* stage increased significantly when the *HA*

temperature was increased, with the first peak of the corresponding curve increasing from 0.133%/min to 0.303%/min. This is because the *IMC* of walnuts is high, and increasing the drying temperature decreases the relative humidity around the walnuts, and the increased humidity difference between walnuts and their surroundings, which leads to a faster migration of water [45,46].

**Table 2.** Moisture content ($MC_E$), drying times ($t_{HAD}$, $t_{MVD}$, $t_T$), and drying rates ($DR_{HAD}$, $DR_{MVD}$, $DR_{AVG}$) of walnuts subjected to *HA-MWD*.

| Test No. | *HAD* Stage | | *MVD* Stage | | $MC_E$ | $t_T$ | $DR_{AVG}$ |
|---|---|---|---|---|---|---|---|
| | $t_{HAD}$ | $DR_{HAD}$ | $t_{MVD}$ | $DR_{MVD}$ | | | |
| 1 | 195 ± 4 | 0.064 ± 0.001 | 30 ± 1 | 0.976 ± 0.006 | 7.99 ± 0.5 | 225 ± 5 | 0.516 ± 0.006 |
| 2 | 135 ± 4 | 0.085 ± 0.001 | 30 ± 1 | 0.971 ± 0.006 | 7.95 ± 0.5 | 165 ± 4 | 0.579 ± 0.006 |
| 3 | 75 ± 3 | 0.152 ± 0.001 | 28 ± 1 | 1.030 ± 0.008 | 7.80 ± 0.5 | 103 ± 4 | 0.669 ± 0.006 |
| 4 | 60 ± 3 | 0.191 ± 0.001 | 25 ± 1 | 1.138 ± 0.008 | 7.88 ± 0.5 | 85 ± 3 | 0.759 ± 0.006 |
| 5 | 50 ± 3 | 0.225 ± 0.001 | 27 ± 1 | 1.120 ± 0.008 | 7.58 ± 0.5 | 77 ± 3 | 0.758 ± 0.006 |
| 6 | 45 ± 3 | 0.125 ± 0.001 | 37 ± 1 | 1.032 ± 0.008 | 7.90 ± 0.5 | 82 ± 3 | 0.862 ± 0.006 |
| 7 | 135 ± 4 | 0.085 ± 0.001 | 30 ± 1 | 0.971 ± 0.006 | 7.95 ± 0.5 | 165 ± 4 | 0.528 ± 0.006 |
| 8 | 270 ± 5 | 0.068 ± 0.001 | 26 ± 1 | 0.842 ± 0.006 | 7.95 ± 0.5 | 296 ± 5 | 0.304 ± 0.005 |
| 9 | 470 ± 6 | 0.061 ± 0.001 | 22 ± 1 | 0.576 ± 0.006 | 7.98 ± 0.5 | 492 ± 6 | 0.164 ± 0.004 |
| 10 | 670 ± 8 | 0.054 ± 0.001 | 15 ± 0.5 | 0.472 ± 0.005 | 7.89 ± 0.5 | 685 ± 8 | 0.100 ± 0.004 |
| 11 | 135 ± 4 | 0.085 ± 0.001 | 125 ± 3 | 0.268 ± 0.004 | 7.68 ± 0.5 | 260 ± 5 | 0.181 ± 0.004 |
| 12 | 135 ± 4 | 0.085 ± 0.001 | 55 ± 2 | 0.741 ± 0.006 | 7.59 ± 0.5 | 190 ± 4 | 0.430 ± 0.006 |
| 13 | 135 ± 4 | 0.085 ± 0.001 | 30 ± 1 | 0.971 ± 0.006 | 7.95 ± 0.5 | 165 ± 4 | 0.528 ± 0.006 |
| 14 | 135 ± 4 | 0.085 ± 0.001 | 20 ± 1 | 1.746 ± 0.01 | 7.66 ± 0.5 | 155 ± 4 | 0.915 ± 0.006 |
| 15 | 135 ± 4 | 0.085 ± 0.001 | 13 ± 0.5 | 2.193 ± 0.01 | 7.99 ± 0.5 | 148 ± 4 | 1.077 ± 0.008 |
| 16 | 135 ± 4 | 0.085 ± 0.001 | 270 ± 4 | 0.114 ± 0.004 | 7.96 ± 0.5 | 405 ± 6 | 0.102 ± 0.008 |
| 17 | 135 ± 4 | 0.085 ± 0.001 | 90 ± 2 | 0.450 ± 0.005 | 7.89 ± 0.5 | 225 ± 5 | 0.286 ± 0.005 |
| 18 | 135 ± 4 | 0.085 ± 0.001 | 30 ± 1 | 0.971 ± 0.006 | 7.95 ± 0.5 | 165 ± 4 | 0.528 ± 0.006 |
| 19 | 135 ± 4 | 0.085 ± 0.001 | 19 ± 0.5 | 0.196 ± 0.004 | 7.99 ± 0.5 | 154 ± 4 | 0.967 ± 0.006 |
| 20 | 135 ± 4 | 0.085 ± 0.001 | 15 ± 0.5 | 2.365 ± 0.01 | 8.01 ± 0.5 | 150 ± 4 | 1.082 ± 0.008 |

The test numbers are the same as in Table 1. Symbols: *MC*—moisture content, %; *t*—drying time, min; *DR*—drying rate, %/min. Subscripts: *HAD*—hot air drying; *MVD*—microwave–vacuum drying; *AVG*—average; *E*—equilibrium; *T*—total.

#### 3.1.2. Effect of Moisture Content at the Transition Point on Drying Characteristics

In order to investigate the effects of *MCs* at the transition point of 36, 30, 24, 18 and 14% on the drying characteristics at a *HA* temperature of 60 °C, a microwave power of 600 W and an *MV* thermostatic temperature of 50 °C, the drying curves and drying rate curves of walnuts at different *MC*s at the transition point are shown in Figure 3A,B. As shown in Figure 3A, the *MC* at the transition point was higher and the *HAD* curves were shorter the earlier it entered the *MVD* stage, and the total drying time was shorter. When the *MC* at the transition point increased from 14% to 36%, the total drying time decreased from 685 min to 82 min for walnuts, and the total drying time decreased by 88.03% (Table 2). The results indicate that the use of *MV* in walnut drying was found to be very useful, especially in the final stage of drying.

It can be seen from Figure 3B that an increase in the *MC* at the transition point could effectively improve the drying rate of the *MVD* stage, especially at the beginning of the *MVD* stage. The highest drying rates in the *MVD* stage increased from 0.767%/min to 2.260%/min for walnuts, and the average drying rates in the *HA-MVD* stage increased from 0.100%/min to 0.862%/min (Table 2). This phenomenon is related to the interaction between the absorbing medium and the microwave. Since water is the main radiation-absorbing component, the higher the MC of walnuts, the more microwave energy is absorbed, which increases the kinetic energy in the water molecules and thus accelerates the migration of water [20]. The results show that the sooner the process enters the *MVD* stage, the larger the total drying rate is, and the shorter the total drying time is.

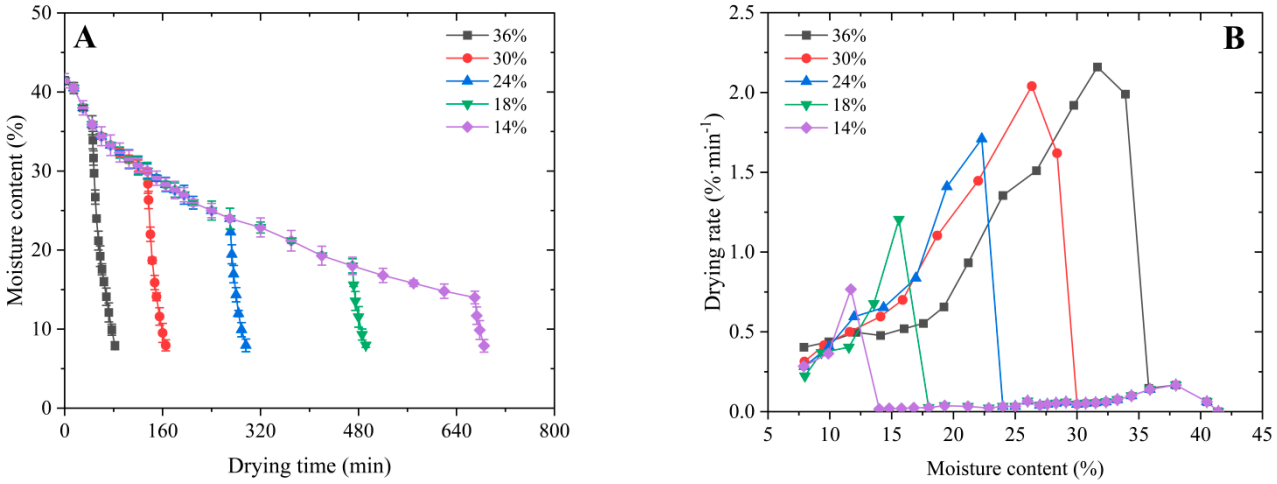



**Figure 3.** (**A**) Drying curves and (**B**) drying rate curves of walnut with different moisture contents at the transition point.

### 3.1.3. Effect of Microwave Power on Drying Characteristics

In order to investigate the effects of microwave powers of 200, 400, 600, 800 and 1000 w on the drying characteristics at a *HA* temperature of 60 °C, an *MC* at the transition point of 30% and an *MV* thermostatic temperature of 50 °C, the drying curves and drying rate curves of walnuts at different microwave power are shown in Figure 4A,B. As shown in Figure 4B, similar to the *HAD* process, when the walnut underwent *MVD*, the drying rate curves of walnuts under different microwave powers successively passed through preheating and falling-rate drying periods. The preheating period of the *MVD* stage corresponds to the stage of internal energy accumulation of walnuts under microwave radiation when the electromagnetic energy was converted into internal thermal energy in the walnut [20]. Although a constant-rate drying period can be expected for a high-moisture food like walnuts, this was not observed in this study, probably because of the single-layer arrangement and because the microwave heating under a vacuum was too fast to provide immediate drying [14,21,47]. With the increase in microwave power, the microwave radiation intensity that the per unit mass of walnuts receives increased. Under this effect, the average drying rates of the walnut for all five power levels (200 W, 400 W, 600 W, 800 W, and 1000 W) significantly increased as follows: 0.181, 0.430, 0.528, 0.915, and 1.077%/min, and microwave drying time decreased (260 min, 190 min, 165 min, 155 min, and 148 min, respectively) (Figure 4A and Table 2). Similar results were found in the drying of hyacinth, where the drying rate increased and the drying time was shortened as the microwave power was increased [25].

It can also be seen from Figure 4B that the effect of microwave power on the drying rate was significantly greater when the *MC* was higher. As the *MC* decreases, the difference in drying rate between different powers gradually decreases, which indicates that the internal mass transfer resistance of the material at low *MC* is significant. Walnuts with a high *MC* and a high dielectric loss factor that is in contact with microwave radiation increases the dipolar rotation in the water molecules, which promotes the absorption of microwave energy and thus accelerates water migration [19,48]. As drying proceeds, the loss of moisture in the walnut reduces the absorption of microwave energy and leads to a decrease in drying rate [19,49]. In addition, it was shown that *MVD* led to a significant increase in the drying rate (almost 3 to 25 times) compared to *HAD* (Table 2). Xong et al. also reported that the drying rate for the *MVD* of cranberries was up to 17 times higher than the drying rate for *HAD* [21].

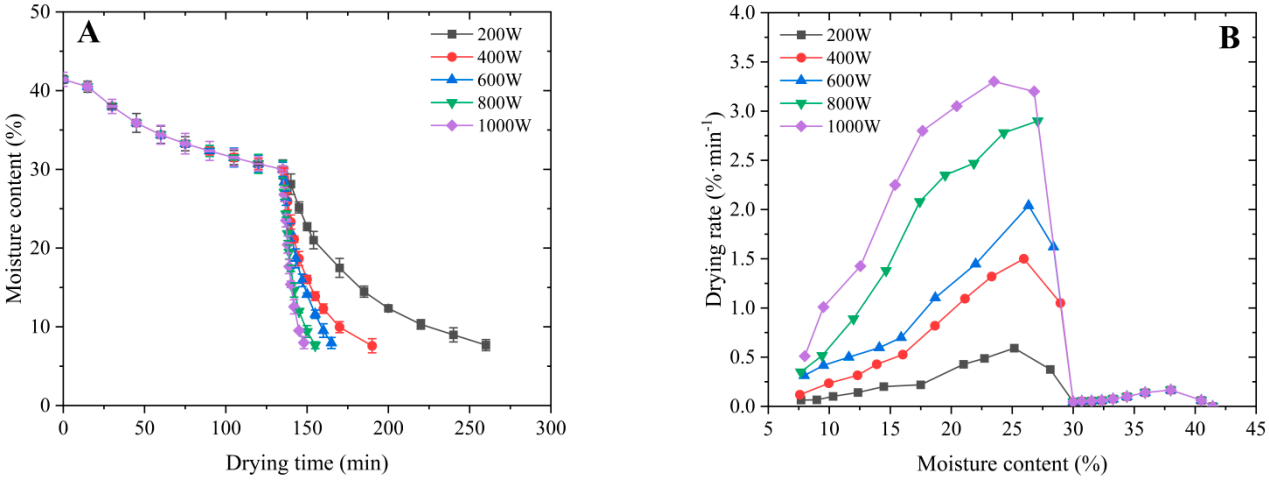



**Figure 4.** (**A**) Drying curves and (**B**) drying rate curves of walnuts at different microwave powers.

#### 3.1.4. Effect of Microwave–Vacuum Thermostatic Temperature on Drying Characteristics

In order to investigate the effects of *MV* thermostatic temperatures of 30, 40, 50, 60, and 70 °C on the drying characteristics at a *HA* temperature of 60 °C, a *MC* at the transition point of 30% and a microwave power of 600 W, the drying curves and drying rate curves of walnuts at different *MV* thermostatic temperatures are shown in Figure 5A,B. As can be seen from Figure 5, since the *HAD* stage of walnut drying had the same conditions, the drying characteristics curves were highly similar to those under the five drying conditions, a characteristic that can also be observed in Figure 4. As shown in Figure 5A, when the *MV* thermostatic temperature is 30 °C, the drying time in the *MVD* stage is the longest, and the total drying time is the longest, which reaches 405 min, while when the *MV* thermostatic temperature rises to 40 °C, the drying time in the *MVD* stage is significantly reduced, and the total drying time is reduced to 225 min (Table 2). These very long drying times indicate that even if *HA-MVD* could be used, a long drying time would be required to complete drying if the *MV* thermostatic temperature is very low. In contrast, when the *MV* thermostatic temperature was 50 °C, 60 °C, and 70 °C, the corresponding drying time was reduced to 150~165 min (Table 2). This indicated that, when *HAD* was converted into higher temperature *MVD* after reaching the *MC* of the transition point, the drying rate improved significantly. Similar results were found for the drying of amaranth seeds [50].

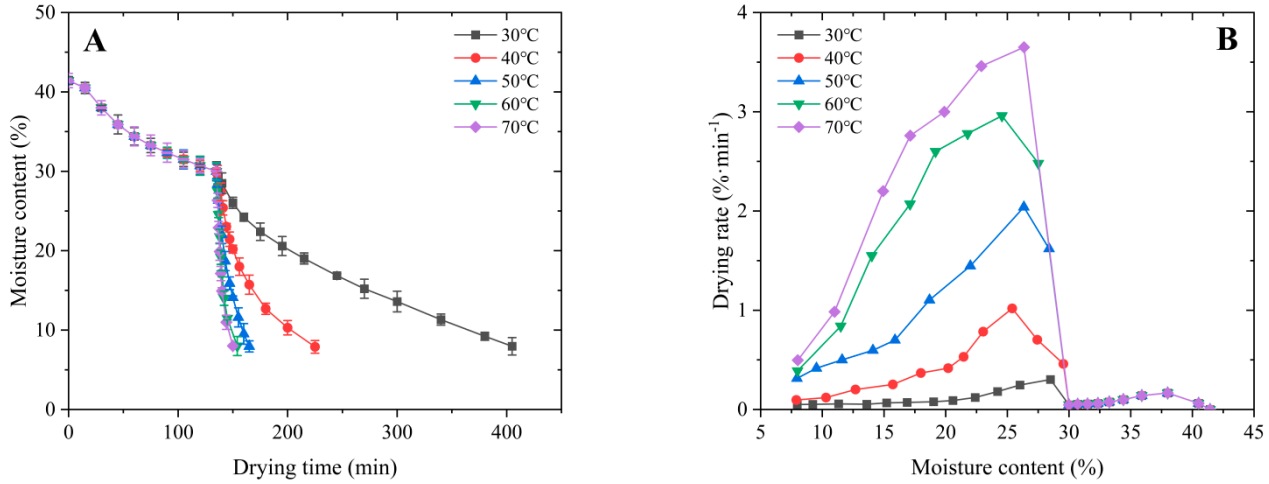



**Figure 5.** (**A**) Drying curves and (**B**) drying rate curves of walnut at different microwave–vacuum thermostatic temperatures.

As shown in Figure 5B, the drying rate increased significantly with increasing *MV* thermostatic temperature in the early period of the *MVD* stage. The average drying rates in the *HA-MVD* stage increased from 0.114%/min to 2.365%/min (Table 2). However, as the amount of water inside the walnut continued to decrease (such as the 12% *MC*), the drying rates under different *MV* thermostatic temperature conditions become smaller and more similar. The moisture migration is affected by the material's own moisture, structure, and other aspects [46]. The moisture migration becomes more difficult due to the moisture protection mechanism of walnut shells [46]. In addition, Figures 2B, 3B, 4B, and 5B show that *HA-MVD* of walnuts occurred mainly in the falling-rate stage, which suggesting that internal moisture diffusion is the main mechanism of moisture transfer of the walnuts [46,51–53]. Hence, Equation (9) was applicable for obtaining the $D_{eff}$ of the walnut under the drying conditions tested in this study.

### 3.2. Effective Moisture Diffusivity

The mechanism of moisture movement within a walnut during the falling-rate period could be represented by the phenomenon of effective moisture diffusion according to a diffusion model [26,29,30]. The $D_{eff}$s were calculated from Equation (9) at different *MC*s according to the drying curves. Figure 6 shows the changes of $D_{eff}$s of a walnut with an *MC* under the *HA-MVD* process at the different drying conditions. The results show that the trends in $D_{eff}$ changes are similar for different *HA* temperatures, different *MCs* at the transition point, different microwave powers, and different *MV* thermostatic temperatures. It was found that the value of $D_{eff}$ dropped sharply with the decrease in the *MC* during the *HAD* stage (corresponding to the high moisture ranges), and when the drying entered the *MVD* stage (corresponding to the low moisture ranges), the value of $D_{eff}$ changed slightly with the decrease in *MC*. Such patterns were considered to be a typical phenomenon of liquid water diffusion based on the drying principle [26,32,54]. These results suggest that the $D_{eff}$ cannot be assumed to be constant, especially in the *HAD* stage. These conclusions are consistent with the results reported in Thuwapanichayanan et al. for banana slices [27]. In addition, it was also found that the trends in changes in $D_{eff}$ were consistent with the drying rate in the *HAD* stage, while the trends in changes were not consistent at the *MVD* stage.

As shown in Figure 6A, $D_{eff}$ increases with increases in *HA* temperature. This can be attributed to the fact that a high temperature increases the kinetic energy in the water molecules, thus accelerating moisture diffusion [46]. It was also found that the higher the *HA* temperature, the faster the water diffusion in the subsequent *MVD* process. As thermal energy is moved from the outside to the inside by heat conduction in terms of the *HAD*, the outside is heated faster and has a higher temperature compared to the inside [12]. Therefore, the drying rate on the outside is obviously larger than on the inside when the *HA* temperature increases, resulting in walnuts entering the *MVD* stage with more internal moisture, which may increase its internal temperature and produce more water vapor, and hence provide an additional driving force for the water diffusion [20,32].

As shown in Figure 6B, $D_{eff}$ is very high in the early period of the *HAD* stage, but very low in the later period of the *HAD* stage. It was found that $D_{eff}$ decreases continuously with decreasing *MC* during the *HAD* process, while switching to *MVD* at any *MCs* at the transition point could truncate the decrease in $D_{eff}$ and still maintain a high value until the end of drying. The results showed that, despite the fact that walnut samples were dried with *HAD* up to a certain extent, the ensuing *MVD* had a strong positive effect on their water diffusion. This is due to the high penetration power and volumetric heating of *MD*. Specifically, microwaves rapidly penetrate walnut shells, providing the energy required for internal water diffusion. Volumetric heating of intracellular water creates a high pressure within the cell walls, which accelerates water diffusion [14,15,18,21]. The results showed that the application of *MVD* in the final stage of drying could rapidly increase the internal vapor pressure of the walnut, accelerate the diffusion speed of the moisture, and re-enhance the drying rate (Figures 3 and 6B).

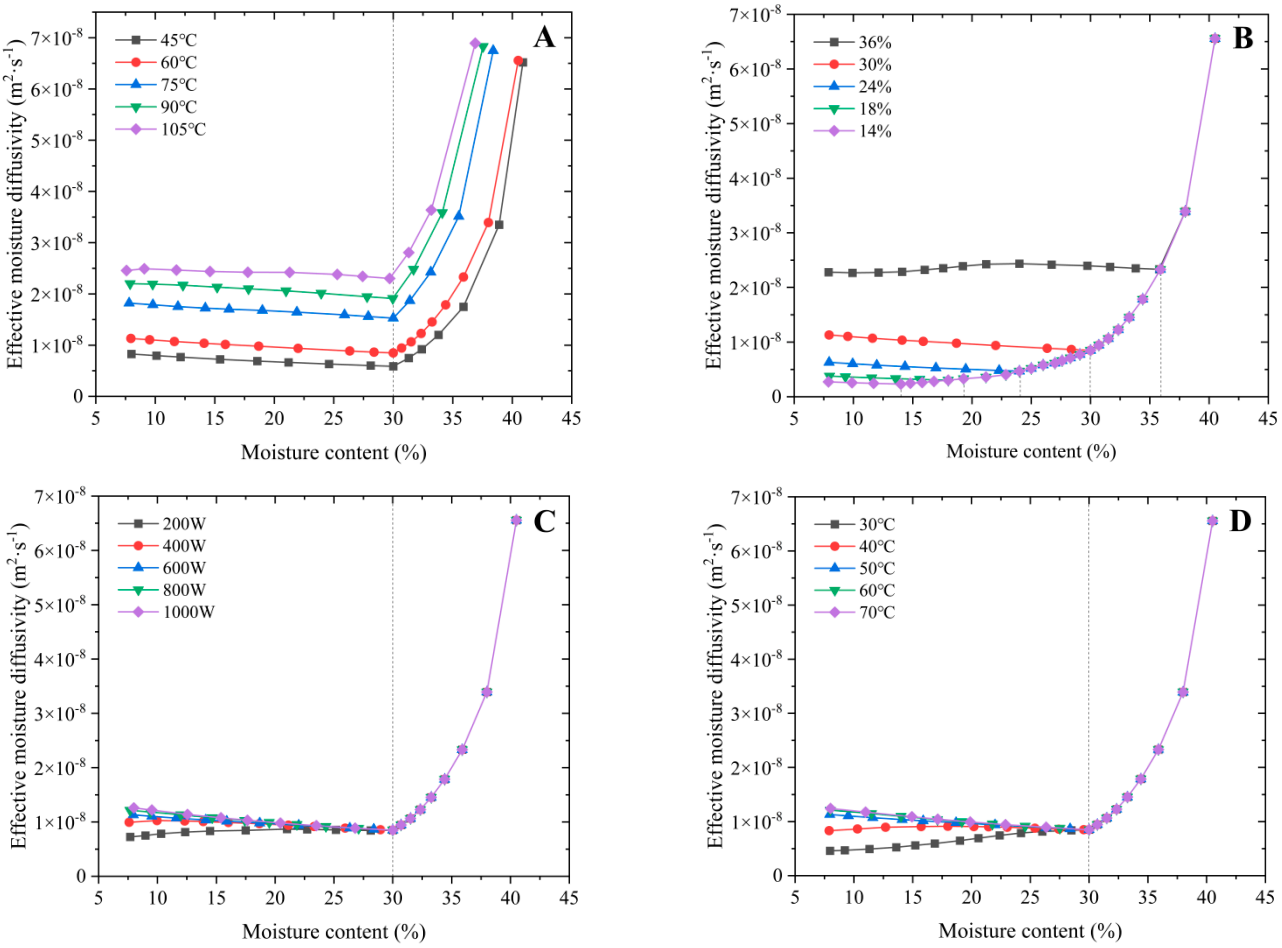



**Figure 6.** Variation in effective moisture diffusivity of walnut with moisture content under *HA-MVD* at different temperatures (45, 60, 75, 90, and 105 °C) (**A**) and different moisture contents at the transition point (36, 30, 24, 18, and 14%) (**B**) and different microwave powers (200, 400, 600, 800, and 1000 W) (**C**) and different microwave–vacuum thermostatic temperatures (30, 40, 50, 60, and 70 °C) (**D**). Note that the position of the dotted line indicates the moisture content at the transition point.

It can be seen from Figure 6C that the $D_{eff}$ increases with an increase in microwave power. The increase is attributed to the significant effect of microwave power in generating molecular motion, increasing the water vapor pressure inside the material, and decreasing the equilibrium *MC* at the material's surfaces [21,25]. It was found that the $D_{eff}$ decreases with decreasing *MC* at a microwave power of 200 W, while it increases slightly with decreasing *MC* at microwave powers of 400, 600, 800 and 1000 W. It can be seen from Figure 6D that a higher *MV* thermostatic temperature may cause the moisture molecules in the walnut to evaporate faster, thus resulting in a faster decrease in *MC* and a correspondingly higher value of $D_{eff}$. It was also found that the $D_{eff}$ decreases with decreasing *MC* at *MV* thermostatic temperatures of 30 and 40 °C, while it increases slightly with decreasing *MC* at *MV* thermostatic temperatures of 50, 60, and 70 °C. This phenomenon is related to the drying time in the *MVD* stage [20,25]. Specifically, when the microwave power was 200 W and the *MV* thermostatic temperature was 30 and 40 °C, the drying time was very long (225–405 min) and $D_{eff}$ decreased with decreasing *MC*, while when the microwave power was 400, 600, 800, and 1000 W and the *MV* thermostatic temperature was 50, 60, and 70 °C, the drying time was shorter (148–190 min) and $D_{eff}$ increased with decreasing *MC* (Table 2). In addition, comparing Figure 6C,D, the moisture diffusion law under different *MV* thermostatic temperatures is similar to that under different microwave powers, and the effect of *MV* thermostatic temperature on the moisture diffusion characteristics was greater than that of microwave power. The values of $D_{eff}$ found in this study were in the

range of $2.33 \times 10^{-9}$ m$^2$/s to $6.89 \times 10^{-8}$ m$^2$/s, which is a typical range for drying food and agricultural materials [25–30,32,36–38,40,42,43,52,55,56].

The $D_{eff,ave}$ values of walnuts under different drying conditions were calculated using Equation (10) and are summarised in Table 3. Figure 7 shows the effect of different drying conditions on the $D_{eff,ave}$ of walnuts. It was found that, as the *HA* temperature increased from 45 to 105 °C, the value of $D_{eff,ave}$ for walnut increased linearly from $1.386 \times 10^{-8}$ to $2.922 \times 10^{-8}$ m$^2$/s (Figure 7A); as the *MC* at the transition point increased from 14 to 36%, the value of $D_{eff,ave}$ for the walnut increased slowly and then rapidly, ranging from $1.005 \times 10^{-8}$ to $2.679 \times 10^{-8}$ m$^2$/s (Figure 7B); as the microwave power increased from 200 to 1000 W, the value of $D_{eff,ave}$ for the walnut increased linearly from $1.463 \times 10^{-8}$ to $1.655 \times 10^{-8}$ m$^2$/s (Figure 7C); as the *MV* thermostatic temperature increased from 30 to 70 °C, the value of $D_{eff,ave}$ for the walnut increased rapidly and then slowly, ranging from $1.297 \times 10^{-8}$ to $1.686 \times 10^{-8}$ m$^2$/s (Figure 7D). Comparing Figure 7A–D, *HA* temperature and the *MC* at the transition point have a greater effect on the $D_{eff,ave}$ than the microwave power and *MV* thermostatic temperature, which suggests that the $D_{eff,ave}$ is more sensitive to increases in the *HA* temperature and the *MC* at the transition point than to increases in microwave power and *MV* thermostatic temperature during the *HA-MVD* process of walnut.

**Table 3.** Regression coefficients for moisture diffusivity model at different drying conditions.

| Test No. | $D_{eff,ave}$ | *A* | *B* | *C* | *D* | $R^2$ | *RSS* |
|---|---|---|---|---|---|---|---|
| 1 | $1.386 \times 10^{-8}$ | $7.83 \times 10^{-12}$ | $-4.69 \times 10^{-10}$ | $8.40 \times 10^{-9}$ | $-3.62 \times 10^{-8}$ | 0.944 | $9.120 \times 10^{-17}$ |
| 2 | $1.591 \times 10^{-8}$ | $7.69 \times 10^{-12}$ | $-4.52 \times 10^{-10}$ | $7.90 \times 10^{-9}$ | $-2.98 \times 10^{-8}$ | 0.957 | $8.530 \times 10^{-17}$ |
| 3 | $2.239 \times 10^{-8}$ | $9.12 \times 10^{-12}$ | $-5.19 \times 10^{-10}$ | $8.79 \times 10^{-9}$ | $-2.63 \times 10^{-8}$ | 0.951 | $1.239 \times 10^{-16}$ |
| 4 | $2.636 \times 10^{-8}$ | $1.00 \times 10^{-11}$ | $-5.67 \times 10^{-10}$ | $9.57 \times 10^{-9}$ | $-2.59 \times 10^{-8}$ | 0.960 | $1.427 \times 10^{-16}$ |
| 5 | $2.922 \times 10^{-8}$ | $9.79 \times 10^{-12}$ | $-5.43 \times 10^{-10}$ | $9.01 \times 10^{-9}$ | $-1.92 \times 10^{-8}$ | 0.951 | $1.977 \times 10^{-16}$ |
| 6 | $2.679 \times 10^{-8}$ | $6.59 \times 10^{-12}$ | $-4.14 \times 10^{-10}$ | $7.86 \times 10^{-9}$ | $-2.08 \times 10^{-8}$ | 0.820 | $3.399 \times 10^{-16}$ |
| 7 | $1.591 \times 10^{-8}$ | $7.69 \times 10^{-12}$ | $-4.52 \times 10^{-10}$ | $7.90 \times 10^{-9}$ | $-2.98 \times 10^{-8}$ | 0.957 | $1.427 \times 10^{-16}$ |
| 8 | $1.210 \times 10^{-8}$ | $6.87 \times 10^{-12}$ | $-3.97 \times 10^{-10}$ | $7.01 \times 10^{-9}$ | $-3.10 \times 10^{-8}$ | 0.963 | $1.515 \times 10^{-16}$ |
| 9 | $1.083 \times 10^{-8}$ | $6.42 \times 10^{-12}$ | $-3.67 \times 10^{-10}$ | $6.53 \times 10^{-9}$ | $-3.12 \times 10^{-8}$ | 0.960 | $1.767 \times 10^{-16}$ |
| 10 | $1.005 \times 10^{-8}$ | $6.17 \times 10^{-12}$ | $-3.51 \times 10^{-10}$ | $6.31 \times 10^{-9}$ | $-3.17 \times 10^{-8}$ | 0.958 | $1.919 \times 10^{-16}$ |
| 11 | $1.463 \times 10^{-8}$ | $7.86 \times 10^{-12}$ | $-4.71 \times 10^{-10}$ | $8.58 \times 10^{-9}$ | $-3.78 \times 10^{-8}$ | 0.958 | $1.512 \times 10^{-16}$ |
| 12 | $1.538 \times 10^{-8}$ | $7.74 \times 10^{-12}$ | $-4.58 \times 10^{-10}$ | $8.12 \times 10^{-9}$ | $-3.22 \times 10^{-8}$ | 0.956 | $1.507 \times 10^{-16}$ |
| 13 | $1.591 \times 10^{-8}$ | $7.69 \times 10^{-12}$ | $-4.52 \times 10^{-10}$ | $7.90 \times 10^{-9}$ | $-2.98 \times 10^{-8}$ | 0.957 | $1.427 \times 10^{-16}$ |
| 14 | $1.611 \times 10^{-8}$ | $7.80 \times 10^{-12}$ | $-4.58 \times 10^{-10}$ | $7.94 \times 10^{-9}$ | $-2.85 \times 10^{-8}$ | 0.956 | $1.450 \times 10^{-16}$ |
| 15 | $1.655 \times 10^{-8}$ | $7.88 \times 10^{-12}$ | $-4.63 \times 10^{-10}$ | $8.02 \times 10^{-9}$ | $-2.88 \times 10^{-8}$ | 0.958 | $1.353 \times 10^{-16}$ |
| 16 | $1.297 \times 10^{-8}$ | $7.38 \times 10^{-12}$ | $-4.40 \times 10^{-10}$ | $8.15 \times 10^{-9}$ | $-3.96 \times 10^{-8}$ | 0.954 | $1.791 \times 10^{-16}$ |
| 17 | $1.465 \times 10^{-8}$ | $7.50 \times 10^{-12}$ | $-4.37 \times 10^{-10}$ | $7.84 \times 10^{-9}$ | $-3.51 \times 10^{-8}$ | 0.958 | $1.493 \times 10^{-16}$ |
| 18 | $1.591 \times 10^{-8}$ | $7.69 \times 10^{-12}$ | $-4.52 \times 10^{-10}$ | $7.90 \times 10^{-9}$ | $-2.98 \times 10^{-8}$ | 0.957 | $1.427 \times 10^{-16}$ |
| 19 | $1.638 \times 10^{-8}$ | $7.96 \times 10^{-12}$ | $-4.72 \times 10^{-10}$ | $8.29 \times 10^{-9}$ | $-3.12 \times 10^{-8}$ | 0.958 | $1.380 \times 10^{-16}$ |
| 20 | $1.687 \times 10^{-8}$ | $8.02 \times 10^{-12}$ | $-7.74 \times 10^{-10}$ | $8.25 \times 10^{-9}$ | $-3.03 \times 10^{-8}$ | 0.960 | $1.290 \times 10^{-16}$ |

The highest and lowest $D_{eff,ave}$ values for the *HA-MVD* of walnuts were $1.005 \times 10^{-8}$ m$^2$/s and $2.922 \times 10^{-8}$ m$^2$/s, respectively. For drying walnuts with a *HA* dryer, Chen et al. reported $D_{eff,ave}$ values in the range of $1.51 \times 10^{-9}$ to $9.28 \times 10^{-9}$ m$^2$/s and $1.13 \times 10^{-9}$ to $2.85 \times 10^{-9}$ m$^2$/s for the walnut shell and kernel, respectively [32]. The results show that the *HA-MVD* could raise the $D_{eff}$ by one order of magnitude compared to the *HAD*. This indicates that the replacement of *HA* with *MV* in the final stage of drying walnuts greatly improved the diffusivity of internal moisture. According to the drying theory, internal moisture diffusivity is controlled by a combination of heat and moisture diffusion. Heat diffusion is water transfer caused by a temperature gradient inside the material, while moisture diffusion is water transfer caused by a moisture gradient in the material. If the moisture diffusion and heat diffusion are in the same direction, then heat diffusion catalyses moisture diffusion and increases the internal moisture diffusiv-

ity; conversely, heat diffusion hinders moisture diffusion [20,57]. During *HAD*, thermal energy is translated from the outside to the inside of the particle by thermal conduction, while moisture is moved from the inside to the surface of the particle due to moisture concentration differences [12,32]. Therefore, heat diffusion of the material increases the resistance to internal moisture diffusion [20,57]. In the *MVD* process, heat is generated inside the particles. In this case, both heat and moisture diffusion are transported from the inside to the outside, which contributes to moisture diffusion [14,19,20]. Meanwhile, the accumulation of internal heat sources can generate vapor pressure inside the particle, which promotes moisture diffusion [15,18,21]. In addition, the walnut structure is prone to producing more open pores under the combined effect of microwave and vacuum, which increases the diffusion channels and reduces the diffusion resistance, thereby accelerating water diffusion [52].

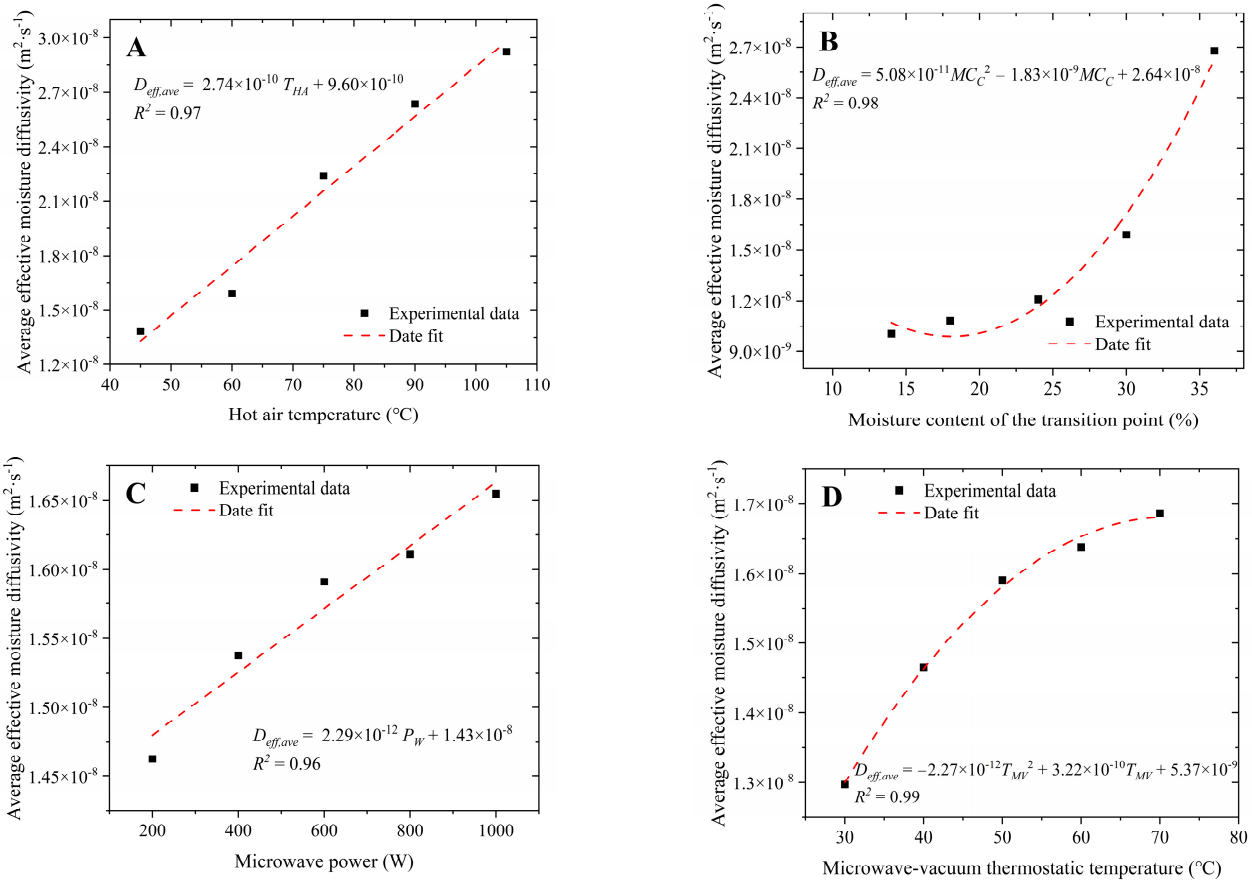



**Figure 7.** Effect of hot air temperature (**A**), moisture content at the transition point (**B**), microwave power (**C**), and microwave–vacuum thermostatic temperature (**D**) on the $D_{eff,ave}$ of walnut.

### *3.3. Model Development for Effective Moisture Diffusivity*

$D_{eff}$ models for walnuts under *HA-MVD* were developed using a non-linear regression method. The values of *A*, *B*, *C*, and *D* in the model, along with the values of $R^2$ and *RSS*, are shown in Table 3. The results show that the dynamic evolution of $D_{eff}$ during the walnut *HA-MVD* process could be accurately represented by a third-order regression model. To include the influence of different drying conditions in the $D_{eff}$ models, regression parameters were fitted using polynomial equations. These polynomial equations are shown in Equations (14)–(29). The $R^2$ values ranged between 0.943 and 0.999, which indicated the high performance of the regression fittings.

At a *MC* at the transition point of 30%, a microwave power of 600 W, and an *MV* thermostatic temperature of 50 °C:

$$A = -6.6 \times 10^{-17} {T_{HA}}^3 + 1.5 \times 10^{-14} {T_{HA}}^2 - 9.8 \times 10^{-13} T_{HA} + 2.9 \times 10^{-11} (R^2 = 0.992) \quad (14)$$

$$B = 3.9 \times 10^{-15} {T_{HA}}^3 - 8.6 \times 10^{-13} {T_{HA}}^2 + 5.9 \times 10^{-11} T_{HA} - 1.7 \times 10^{-9} (R^2 = 0.996) \quad (15)$$

$$C = -6.7 \times 10^{-14} {T_{HA}}^3 + 1.5 \times 10^{-11} {T_{HA}}^2 - 1.1 \times 10^{-9} T_{HA} + 3.2 \times 10^{-8} (R^2 = 0.999) \quad (16)$$

$$D = 2.3 \times 10^{-13} {T_{HA}}^3 - 5.2 \times 10^{-11} {T_{HA}}^2 + 4.0 \times 10^{-9} T_{HA} - 1.3 \times 10^{-7} (R^2 = 0.991) \quad (17)$$

At a *HA* temperature of 60 °C, a microwave power of 600 W, and an *MV* thermostatic temperature of 50 °C:

$$A = -9.6 \times 10^{-16} {MC_C}^3 + 6.5 \times 10^{-14} {MC_C}^2 - 1.3 \times 10^{-12} MC_C + 1.5 \times 10^{-11} (R^2 = 0.948) \quad (18)$$

$$B = 4.8 \times 10^{-14} {MC_C}^3 - 3.4 \times 10^{-12} {MC_C}^2 + 6.9 \times 10^{-11} MC_C - 7.9 \times 10^{-10} (R^2 = 0.969) \quad (19)$$

$$C = -5.4 \times 10^{-13} {MC_C}^3 + 3.9 \times 10^{-11} {MC_C}^2 - 8.1 \times 10^{-10} MC_C + 1.2 \times 10^{-8} (R^2 = 0.988) \quad (20)$$

$$D = 3.7 \times 10^{-12} {MC_C}^3 - 2.4 \times 10^{-10} {MC_C}^2 + 4.9 \times 10^{-9} MC_C - 6.5 \times 10^{-8} (R^2 = 0.997) \quad (21)$$

At a *HA* temperature of 60 °C, an *MC* at the transition point of 30%, and an *MV* thermostatic temperature of 50 °C:

$$A = -1.0 \times 10^{-21} {P_W}^3 + 2.9 \times 10^{-18} {P_W}^2 - 2.1 \times 10^{-15} P_W + 8.2 \times 10^{-12} (R^2 = 0.956) \quad (22)$$

$$B = 8.3 \times 10^{-20} {P_W}^3 - 2.4 \times 10^{-16} {P_W}^2 + 1.9 \times 10^{-13} P_W - 5.0 \times 10^{-10} (R^2 = 0.977) \quad (23)$$

$$C = -2.1 \times 10^{-18} {P_W}^3 + 6.1 \times 10^{-15} {P_W}^2 - 5.5 \times 10^{-12} P_W + 9.5 \times 10^{-9} (R^2 = 0.997) \quad (24)$$

$$D = 1.7 \times 10^{-17} {P_W}^3 - 5.3 \times 10^{-14} {P_W}^2 + 5.4 \times 10^{-11} P_W - 4.7 \times 10^{-8} (R^2 = 0.998) \quad (25)$$

At a *HA* temperature of 60 °C, an *MC* at the transition point of 30%, and a microwave power of 600 W:

$$A = -2.3 \times 10^{-17} {T_{MV}}^3 + 3.5 \times 10^{-15} {T_{MV}}^2 - 1.5 \times 10^{-13} T_{MV} + 9.3 \times 10^{-12} (R^2 = 0.996) \quad (26)$$

$$B = 2.9 \times 10^{-15} {T_{MV}}^3 - 4.5 \times 10^{-13} {T_{MV}}^2 + 2.1 \times 10^{-11} T_{MV} - 7.4 \times 10^{-10} (R^2 = 0.998) \quad (27)$$

$$C = -6.7 \times 10^{-14} {T_{MV}}^3 + 1.1 \times 10^{-11} {T_{MV}}^2 - 5.4 \times 10^{-10} T_{MV} + 1.6 \times 10^{-8} (R^2 = 0.957) \quad (28)$$

$$D = 1.3 \times 10^{-13} {T_{MV}}^3 - 2.9 \times 10^{-11} {T_{MV}}^2 + 2.1 \times 10^{-9} T_{MV} - 8.1 \times 10^{-8} (R^2 = 0.943) \quad (29)$$

where, $T_{HA}$ is the hot air temperature (°C); $MC_C$ is the moisture content at the transition point (%); $P_W$ is the microwave power (W); and $T_{MV}$ is the microwave–vacuum thermostatic temperature (°C).

To verify whether the $D_{eff}$ model can accurately predict the evolution of moisture diffusion characteristics of walnuts during the *HA-MVD* process, Figure 8 shows a comparison of experimental $D_{eff}$ and the $D_{eff}$ predicted by the $D_{eff}$ model. According to the literature, if the curves of the experimental and predicted values are approximately at a 45° angle, it means that the predicted values represent the experimental values well [52]. As can be seen from Figure 8, the $D_{eff}$ model provided a good conformity between experimental and predicted $D_{eff}$ during the *HA-MVD* processes of walnuts. These data points are banded line plots at an angle of approximately 45°, which suggests that the $D_{eff}$ model is able to make good predictions of the dynamic change of $D_{eff}$ during the walnut *HA-MVD* processes under different drying conditions. Meanwhile, the 45° banded line graphs also show the accuracy of the proposed third-order polynomial functions, and these can be embedded in future FEM simulations to model the water loss of walnuts during *HA-MVD*, which could

provide a theoretical basis for elucidating the water loss mechanism of walnuts during *HA-MVD*.

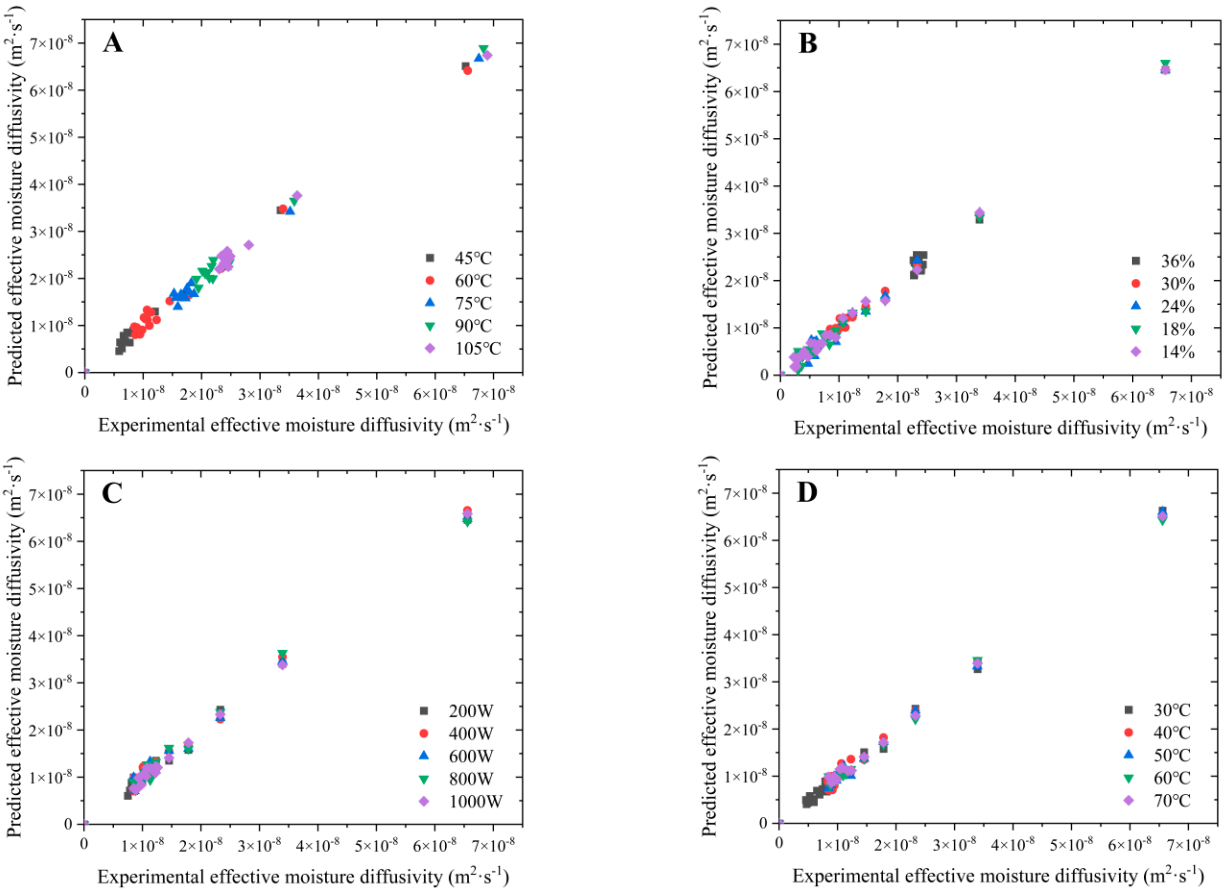



**Figure 8.** Comparison of experimental and predicted $D_{eff}$ from $D_{eff}$ model at different temperatures (**A**), different moisture contents at the transition point (**B**), different microwave powers (**C**), and different microwave–vacuum thermostatic temperatures (**D**).

## 4. Conclusions

A *HA-MAD* system was established to investigate the drying characteristics and moisture diffusion properties of walnuts and to develop a $D_{eff}$ model. Based on the experimental findings, several key conclusions were drawn:

(1) The *HA-MVD* of walnut occurred mainly in the falling-rate stage. The average drying rate for *MVD* was up to 3 to 25 times higher than the average drying rate for *HAD*. The total drying time shorted and the average drying rate increased with increasing *HA* temperature, *MC* at the transition point, microwave power, and *MV* thermostatic temperature.

(2) The value of $D_{eff}$ dropped continuously with the decrease in *MC* in the *HAD* stage, while switching to the *MVD* stage could truncate the decrease in $D_{eff}$ and still maintain at a high value until the end of drying.

(3) The values of $D_{eff}$ for walnut ranged from $2.33 \times 10^{-9}$ $m^2/s$ to $6.89 \times 10^{-8}$ $m^2/s$. The *HA* temperature and *MC* at the transition point have a greater effect on the $D_{eff}$ than the microwave power and *MV* thermostatic temperature. The replacement of *HAD* with *MVD* in the final stage of the drying of walnuts could raise the $D_{eff}$ by one order of magnitude.

(4) The third-order polynomial prediction model of $D_{eff}$ related to the sample *MC* and drying conditions could accurately describe the dynamic change of $D_{eff}$ of walnut during the *HA-MVD* process.

**Author Contributions:** Conceptualization, X.F. and H.Z.; methodology, Y.T. and H.L.; software, X.M. and L.L.; investigation, X.M.; resources, X.F., H.Z. and Y.Z.; data curation, X.M. and L.L.; writing—original draft preparation, X.M.; writing—review and editing, X.M., L.L. and X.F.; visualization, Y.Z.; supervision, H.L.; project administration, H.Z. All authors have read and agreed to the published version of the manuscript.

**Funding:** This work has been financially supported and encouraged by the Shishi Science and Technology Program (Grant No. 2021ZB01, 2022ZB05, 2022ZB07), Bingtuan Science and Technology Program (Grant No. 2022CB08, 2018CB014), Modern Agricultural Engineering Key Laboratory at Universities of Education Department of Xinjiang Uygur Autonomous Region (Grant No. TDNG2022101).

**Institutional Review Board Statement:** Not applicable.

**Data Availability Statement:** The data presented in this study are available on request from the corresponding author.

**Acknowledgments:** The authors thank Haipeng Lan from Tarim University for thesis supervision. The authors are grateful to the anonymous reviewers for their comments.

**Conflicts of Interest:** The authors declare no conflicts of interest.

## References

1. Erfani, A.; Pirouzifard, M.K.; Almasi, H.; Gheybi, N.; Pirsa, S. Application of cellulose plate modified with encapsulated cinnamomum zelanicum essential oil in active packaging of walnut kernel. *Food Chem.* **2022**, *381*, 132246. [CrossRef] [PubMed]
2. Man, X.L.; Li, L.; Zeng, Y.; Tang, Y.R.; Yang, J.L.; Fan, X.W.; Zhang, Y.C.; Zhang, H.; Su, G.G.; Wang, J.P. Mechanical impact characteristics of hollow shell granule based on continuous damage theory. *Powder Technol.* **2023**, *429*, 118946. [CrossRef]
3. Liu, M.Z.; Li, C.H.; Cao, C.M.; Wang, L.Q.; Li, X.P.; Che, J.; Yang, H.M.; Zhang, X.W.; Zhao, H.Y.; He, G.Z.; et al. Walnut fruit processing equipment: Academic insights and perspectives. *Food Eng. Rev.* **2021**, *13*, 822–857. [CrossRef]
4. Fu, M.; Qu, Q.; Yang, X.; Zhang, X. Effect of intermittent oven drying on lipid oxidation, fatty acids composition and antioxidant activities of walnut. *LWT-Food Sci. Technol.* **2016**, *65*, 1126–1132. [CrossRef]
5. Mao, Y.X.; Wang, P.H.; Wu, Y.; Hou, L.X.; Wang, S.J. Effects of various radio frequencies on combined drying and disinfestation treatments for in-shell walnuts. *LWT-Food Sci. Technol.* **2021**, *144*, 111246. [CrossRef]
6. Qu, Q.; Yang, X.; Fu, M.; Chen, Q.; Zhang, X.; He, Z.; Qiao, X. Effects of three conventional drying methods on the lipid oxidation, fatty acids composition, and antioxidant activities of walnut (*Juglans regia* L.). *Dry. Technol.* **2016**, *34*, 822–829. [CrossRef]
7. Zhou, X.; Gao, H.; Mitcham, E.J.; Wang, S. Comparative analyses of three dehydration methods on drying characteristics and oil quality of in-shell walnuts. *Dry. Technol.* **2018**, *36*, 477–490. [CrossRef]
8. Chen, C.; Pan, Z.L. Postharvest processing of tree nuts: Current status and future prospects-A comprehensive review. *Compr. Rev. Food Sci. Food Saf.* **2022**, *21*, 1702–1731. [CrossRef]
9. Dolgun, G.K.; Aktas, M.; Dolgun, E.C. Infrared convective drying of walnut with energy-exergy perspective. *J. Food Eng.* **2021**, *306*, 110638. [CrossRef]
10. Zhu, D.Q.; Ma, J.; Jiang, R.; Yuan, J.H.; Wang, C.X.; Zhu, H. Parameter optimization of hickory nut drying by phased varying power microwave. *Trans. CSAE* **2016**, *32*, 268–274. [CrossRef]
11. Chen, C.; Zhang, W.P.; Venkitasamy, C.; Khir, R.; McHugh, T.; Pan, Z.L. Walnut structure and its influence on the hydration and drying characteristics. *Dry. Technol.* **2019**, *38*, 975–986. [CrossRef]
12. Chen, C.; Upadhyaya, S.; Khir, R.; Pan, Z.L. Simulation of walnut drying under hot air heating using a nonequilibrium multiphase transfer model. *Dry. Technol.* **2020**, *40*, 987–1001. [CrossRef]
13. Shen, L.Y.; Wang, L.; Zheng, C.Y.; Liu, C.H.; Zhu, Y.; Liu, H.; Liu, C.; Shi, Y.K.; Zheng, X.Z.; Xu, H. Continuous microwave drying of germinated brown rice: Effects of drying conditions on fissure and color, and modeling of moisture content and stress inside kernel. *Dry. Technol.* **2020**, *39*, 669–697. [CrossRef]
14. Shen, L.Y.; Zhu, Y.; Liu, C.H.; Wang, L.; Liu, H.; Kamruzzaman, M.; Liu, C.; Zhang, Y.P.; Zheng, X.Z. Modelling of moving drying process and analysis of drying characteristics for germinated brown rice under continuous microwave drying. *Biosyst. Eng.* **2020**, *195*, 64–88. [CrossRef]
15. Chen, A.Q.; Achkar, G.E.; Liu, B.; Bennacer, R. Experimental study on moisture kinetics and microstructure evolution in apples during high power microwave drying process. *J. Food Eng.* **2020**, *29*, 110362. [CrossRef]
16. Zielinska, M.; Markowski, M.; Zielinska, D. The effect of freezing on the hot air and microwave vacuum drying kinetics and texture of whole cranberries. *Dry. Technol.* **2019**, *37*, 1714–1730. [CrossRef]
17. Cuccurullo, G.; Metallo, A.; Corona, O.; Cinquanta, L. Comparing different processing methods in apple slice drying. part 1. performance of microwave, hot air and hybrid methods at constant temperatures. *Biosyst. Eng.* **2019**, *188*, 331–344. [CrossRef]
18. Ishibashi, R.; Numata, T.; Tanigawa, H.; Tsuruta, T. In-situ measurements of drying and shrinkage characteristics during microwave vacuum drying of radish and potato. *J. Food Eng.* **2022**, *323*, 110988. [CrossRef]

19. Gonzalez-Cavieres, L.; Pérez-Won, M.; Tabilo-Munizaga, G.; Jara-Quijada, E.; Díaz-Alvarez, R.; Lemus-Mondaca, R. Advances in vacuum microwave drying (VMD) systems for food products. *Trends Food Sci. Technol.* **2021**, *116*, 626–638. [CrossRef]
20. Song, Z.L.; Jing, C.M.; Yao, L.S.; Zhao, X.Q.; Sun, J.; Wang, W.L.; Mao, Y.P.; Ma, C.Y. Coal slime hot air/microwave combined drying characteristics and energy analysis. *Fuel Process Technol.* **2016**, *156*, 491–499. [CrossRef]
21. Zhou, Y.H.; Staniszewska, I.; Liu, Z.L.; Zielinska, D.; Xiao, H.W.; Pan, Z.L.; Nowak, K.W.; Zielinska, M. Microwave-vacuum-assisted drying of pretreated cranberries: Drying kinetics, bioactive compounds and antioxidant activity. *LWT-Food Sci. Technol.* **2021**, *146*, 111464. [CrossRef]
22. Figiel, A. Drying kinetics and quality of beetroots dehydrated by combination of convective and vacuum-microwave methods. *J. Food Eng.* **2010**, *98*, 461–470. [CrossRef]
23. Hu, Q.G.; Zhang, M.; Mujumdar, A.S.; Xiao, G.N.; Sun, J.C. Drying of edamames by hot air and vacuum microwave combination. *J. Food Eng.* **2006**, *77*, 977–982. [CrossRef]
24. Wu, H.H.; Zhu, D.Z.; Zhang, X.X.; Bian, H.; Wang, D.Y.; Zhu, Y.Z. Optimization of processing parameters for microwave vacuum puffing of duck breast after hot-air dehydration. *Food Sci.* **2017**, *38*, 267–273. [CrossRef]
25. Kaveh, M.; Abbaspour-Gilandeh, Y.; Nowacka, M. Optimisation of microwave-rotary drying process and quality parameters of terebinth. *Biosyst. Eng.* **2021**, *208*, 113–130. [CrossRef]
26. Hassini, L.; Azzouz, S.; Peczalski, R.; Belghith, A. Estimation of potato moisture diffusivity from convective drying kinetics with correction for shrinkage. *J. Food Eng.* **2007**, *79*, 47–56. [CrossRef]
27. Thuwapanichayanan, R.; Prachayawarakorn, S.; Kunwisawa, J.; Soponronnarit, S. Determination of effective moisture diffusivity and assessment of quality attributes of banana slices during drying. *LWT-Food Sci. Technol.* **2011**, *44*, 1502–1510. [CrossRef]
28. Khan, M.I.H.; Kumar, C.; Joardder, M.U.H.; Karim, M.A. Determination of appropriate effective diffusivity for different food materials. *Dry. Technol.* **2017**, *35*, 335–346. [CrossRef]
29. Bal, L.M.; Kar, A.; Satya, S.; Naik, S.N. Drying kinetics and effective moisture diffusivity of bamboo shoot slices undergoing microwave drying. *Int. J. Food Sci. Technol.* **2010**, *45*, 2321–2328. [CrossRef]
30. Dadalı, G.; Apar, K.D.; Ozbek, B. Estimation of effective moisture diffusivity of okra for microwave drying. *Dry. Technol.* **2007**, *25*, 1445–1450. [CrossRef]
31. Zeng, Y.; Mao, B.Q.; Jia, F.G.; Han, Y.L.; Li, G.R. Modelling of grain breakage of in a vertical rice mill based on dem simulation combining particle replacement model. *Biosyst. Eng.* **2022**, *215*, 32–48. [CrossRef]
32. Chen, C.; Venkitasamy, C.; Zhang, W.P.; Khir, R.; Upadhyaya, S.; Pan, Z.L. Effective moisture diffusivity and drying simulation of walnuts under hot air. *Int. J. Heat Mass Transf.* **2020**, *150*, 119283. [CrossRef]
33. Xu, W.X.; Song, C.F.; Li, Z.F.; Song, F.H.; Hu, S.G.; Li, J.; Zhu, G.Y.; Raghauan, G.S.V. Temperature gradient control during microwave combined with hot air drying. *Biosyst. Eng.* **2018**, *169*, 175–187. [CrossRef]
34. Nguyen, T.V.L.; Nguyen, Q.D.; Nguyen, P.B.D.; Tran, B.L.; Huynh, P.T. Effects of drying conditions in low-temperature microwaveassisted drying on bioactive compounds and antioxidant activity of dehydrated bitter melon (*Momordica charantia* L.). *Food Sci. Nutr.* **2020**, *8*, 3826–3834. [CrossRef]
35. Ye, J.H.; Xu, C.; Zhang, C.; Zhu, H.C.; Huang, K.M.; Li, Q.; Wang, J.; Zhou, L.; Wu, Y.Y. A hybrid ale/implicit function method for simulating microwave heating with rotating objects of arbitrary shape. *J. Food Eng.* **2021**, *302*, 110551. [CrossRef]
36. Vera, C.M.; Vizcarra, M.G. Concentration-dependent moisture diffusion coefficient estimation in peas drying considering shrinkage: An observer approach. *Biosyst. Eng.* **2022**, *218*, 256–273. [CrossRef]
37. Perazzini, H.; Leonel, A.; Perazzini, M.T.B. Energy of activation, instantaneous energy consumption, and coupled heat and mass transfer modeling in drying of sorghum grains. *Biosyst. Eng.* **2021**, *210*, 181–192. [CrossRef]
38. Wang, H. Effects of different drying methods on drying kinetics, physicochemical properties, microstructure, and energy consumption of potato (*Solanum tuberosum* L.) cubes. *Dry. Technol.* **2020**, *39*, 418–431. [CrossRef]
39. Li, L.; Mao, B.Q.; Zeng, Y.; Tang, Y.R.; Man, X.L.; Fan, X.W.; Zhang, Y.C.; Zhang, H. Experimental study on crack irregularity of hollow shell particle under impact loading. *Powder Technol.* **2023**, *427*, 118704. [CrossRef]
40. Dak, M.; Pareek, N.K. Effective moisture diffusivity of pomegranate arils under going microwave-vacuum drying. *J. Food Eng.* **2014**, *122*, 117–121. [CrossRef]
41. Crank, J. *The Mathematics of Diffusion*; Oxford University Press Inc.: Oxford, UK, 1975.
42. Hassan-Beygi, S.R.; Aghbashlo, M.; Kianmehr, M.H.; Massah, J. Drying characteristics of walnut (*Juglans regia* L.) during convection drying. *Int. Agrophys.* **2009**, *23*, 129–135. [CrossRef]
43. Shi, J.L.; Pan, Z.L.; McHugh, T.H.; Wood, D.; Hirschberg, E.; Olson, D. Drying and quality characteristics of fresh and sugarinfused blueberries dried with infrared radiation heating. *LWT-Food Sci. Technol.* **2008**, *41*, 1962–1972. [CrossRef]
44. Ekezie, F.G.C.; Sun, D.W.; Han, Z.; Cheng, J.H. Microwave-assisted food processing technologies for enhancing product quality and process efficiency: A review of recent developments. *Trends Food Sci. Technol.* **2018**, *67*, 58–69. [CrossRef]
45. Chen, C.; Pan, Z.L. Heat and moisture transfer studies on walnuts during hot air drying in a fixed-bed column dryer. *Appl. Therm. Eng.* **2021**, *199*, 117554. [CrossRef]
46. Lu, Y.J.; Ren, G.Y.; Duan, X.; Zhang, L.D.; Ling, Z.Z. Moisture migration properties and quality changes of fresh in-shell peanuts during hot air drying. *Food Sci.* **2020**, *41*, 86–92. [CrossRef]

47. Sharma, P.; Xiao, H.W.; Zhang, Q.; Sutar, P.P. Intermittent high-power short-time microwave-vacuum treatment combined with steam impingement for effective microbial decontamination of black pepper (piper nigrum). *J. Food Eng.* **2023**, *343*, 111373. [CrossRef]
48. Ma, X.T.; Luo, G.Y.; Li, Z.F.; Raghavan, G.S.V.; Chen, H.Y.; Song, C.F. Microwave power control scheme for potatoes based on dielectric loss factor feedback. *J. Food Eng.* **2020**, *288*, 110134. [CrossRef]
49. Luo, G.Y.; Song, C.F.; Hongjie, P.; Li, Z.F.; Xu, W.X.; Raghavan, G.S.V.; Chen, H.Y.; Jin, G.Y. Optimization of the microwave drying process for potato chips based on the measurement of dielectric properties. *Dry. Technol.* **2019**, *37*, 1329–1339. [CrossRef]
50. Moreno, Á.H.; Aguirre, Á.J.; Maqueda, R.H.; Jiménez, G.J.; Miño, C.T. Effect of temperature on the microwave drying process and the viability of amaranth seeds. *Biosyst. Eng.* **2022**, *215*, 49–66. [CrossRef]
51. Raponi, F.; Moscetti, R.; Chakravartula, S.S.N.; Fidaleo, M.; Massantini, R. Monitoring the hot-air drying process of organically grown apples (cv. gala) using computer vision. *Biosyst. Eng.* **2021**, *223*, 1–13. [CrossRef]
52. Yu, H.M.; Li, H.Y.; Zhang, X.Y.; Wang, H.Y.; Sun, Y. Drying kinetic model of microwave coupled with hot air drying of straw-based nutrient seedling-growing bowl tray. *Trans. CSAM* **2020**, *51*, 339–348. [CrossRef]
53. Chen, C.; Venkitasamy, C.; Zhang, W.P.; Deng, L.Z.; Meng, X.Y.; Pan, Z.L. Effect of step-down temperature drying on energy consumption and product quality of walnuts. *J. Food Eng.* **2020**, *285*, 110105. [CrossRef]
54. Saravacos, G.D.; Maroulis, Z.B. *Food Process Engineering Operations*; CRC Press: Boca Raton, FL, USA, 2013. [CrossRef]
55. Jiang, C.; Wan, F.; Zang, Z.; Zhang, Q.; Ma, G.; Huang, X. Effect of an ultrasound pre-treatment on the characteristics and quality of far-infrared vacuum drying with cistanche slices. *Foods* **2022**, *11*, 866. [CrossRef]
56. Xiao, A.; Ding, C. Effect of electrohydrodynamic (EHD) on drying kinetics and quality characteristics of shiitake mushroom. *Foods* **2022**, *11*, 1303. [CrossRef] [PubMed]
57. Mujumdar, A.S. *Handbook of Industrial Drying*, 4th ed.; CRC Press: Boca Raton, FL, USA, 2014. [CrossRef]


**Disclaimer/Publisher's Note:** The statements, opinions and data contained in all publications are solely those of the individual author(s) and contributor(s) and not of MDPI and/or the editor(s). MDPI and/or the editor(s) disclaim responsibility for any injury to people or property resulting from any ideas, methods, instructions or products referred to in the content.